MOLECULAR AND CELLULAR BIOLOGY, Sept. 2007, p. 6407–6419 Vol. 27, No. 18
0270-7306/07/$08.00+0 doi:10.1128/MCB.00511-07

ASB4 Is a Hydroxylation Substrate of FIH and Promotes Vascular Differentiation via an Oxygen-Dependent Mechanism▽†

James E. Ferguson III,[1,2] Yaxu Wu,[1] Kevin Smith,[1] Peter Charles,[1] Kyle Powers,[1] Hong Wang,[1] and Cam Patterson[1,2,3]*

Department of Pharmacology,[2] Carolina Cardiovascular Biology Center,[1] and Department of Medicine,[3] University of North Carolina, Chapel Hill, North Carolina

Received 23 March 2007/Returned for modification 26 April 2007/Accepted 9 July 2007

The molecular mechanisms of endothelial differentiation into a functional vascular network are incompletely understood. To identify novel factors in endothelial development, we used a microarray screen with differentiating embryonic stem (ES) cells that identified the gene for ankyrin repeat and SOCS box protein 4 (ASB4) as the most highly differentially expressed gene in the vascular lineage during early differentiation. Like other SOCS box-containing proteins, ASB4 is the substrate recognition molecule of an elongin B/elongin C/cullin/Roc ubiquitin ligase complex that mediates the ubiquitination and degradation of substrate protein(s). High levels of ASB4 expression in the embryonic vasculature coincide with drastic increases in oxygen tension as placental blood flow is initiated. However, as vessels mature and oxygen levels stabilize, ASB4 expression is quickly downregulated, suggesting that ASB4 may function to modulate an endothelium-specific response to increasing oxygen tension. Consistent with the hypothesis that ASB4 function is regulated by oxygen concentration, ASB4 interacts with the factor inhibiting HIF1α (FIH) and is a substrate for FIH-mediated hydroxylation via an oxygen-dependent mechanism. Additionally, overexpression of ASB4 in ES cells promotes differentiation into the vascular lineage in an oxygen-dependent manner. We postulate that hydroxylation of ASB4 in normoxia promotes binding to and degradation of substrate protein(s) to modulate vascular differentiation.

Members of the suppressor of cytokine signaling (SOCS) superfamily are E3 ubiquitin ligase components that contain a C-terminal SOCS box and an N-terminal protein-protein binding domain (21, 22). The SOCS box mediates interactions with an elongin B/elongin C/cullin 5/Roc protein complex to constitute a functional E3 ubiquitin ligase complex (19), while the N-terminal protein-protein binding domains recruit substrate proteins to mediate substrate polyubiquitination and proteasome-mediated degradation. In this way, SOCS proteins confer substrate specificity on the E3 ubiquitin ligase complex and are thus tightly regulated at both the transcriptional and posttranslational levels in order to carefully control the steady-state levels of substrate proteins.

Ankyrin repeat (AR) and SOCS box proteins (ASBs) constitute one subclass of the SOCS superfamily and are characterized by variable numbers of N-terminal ARs as substrate-binding domains (reviewed in reference 13). To date, at least 18 family members have been identified in mammals and preliminary functional characterization is currently under way. So far, ASB proteins have been suggested to mediate the ubiquitination of a broad range of target proteins, including tumor necrosis factor receptor II (ASB3) (2), creatine kinase B (ASB9) (5), and adaptor protein with PH and SH2 domains (APS, ASB6) (47). Since ARs function as generic scaffolds for the creation of modular binding sites that mediate interactions with an almost unlimited variety of binding motifs and domains (33, 43), it is not surprising that ASBs interact with and promote the degradation of a wide diversity of target substrate proteins.

Our previous data suggest that ASB4, a poorly characterized member of this family, is highly differentially expressed in the vascular lineage during development (46). Vasculogenesis, or the de novo differentiation of pluripotent stem cells into the vascular lineage during development, is the first stage of blood vessel formation. Vasculogenesis begins shortly after gastrulation in the developing embryo, as cells with vasculogenic potential have been isolated from the primitive-streak region in embryonic day 6.5 (E6.5) mouse embryos (14). These cells, termed hemangioblasts, derive from mesoderm, express brachyury (also referred to as T) and Flk1, and have both vascular potential and hematopoietic potential. Primitive capillary plexi of endothelial cells arise from Flk1-positive populations and are then remodeled in a process similar to that of adult angiogenesis to yield mature lumenized vessels.

A complex combination of genetically preprogrammed molecular signals and external environmental cues are responsible for proper vascular development and remodeling, and an important role of oxygen tension in these processes has recently been discovered. The current understanding of the cellular response to oxygen tension centers around the hypoxia-inducible factor (HIF) family of transcription factors, whose steady-state levels and activity vary inversely with the oxygen concentration (reviewed in references 24, 30, and 39). The factor inhibiting HIF1α (FIH) and the prolyl hydroxylase enzymes

* Corresponding author. Mailing address: Division of Cardiology and Carolina Cardiovascular Biology Center, 8200 Medical Biomolecular Research Building, Chapel Hill, NC 27599-7126. Phone: (919) 843-6477. Fax: (919) 843-4585. E-mail: cpatters@med.unc.edu.

† Supplemental material for this article may be found at http://mcb.asm.org/.

▽ Published ahead of print on 16 July 2007.

(PHDs) catalyze the hydroxylation of the HIF1α and HIF2α subunits on asparagine and proline residues, respectively. FIH-mediated HIF hydroxylation disrupts binding to the transcriptional coactivator p300 and results in decreased transcriptional activity, whereas PHD hydroxylation promotes the binding of von Hippel-Lindau (VHL) protein, a SOCS protein that mediates HIF polyubiquitination and proteasomal degradation through an elongin B/elongin C/Cul2/Roc1 complex. Since these hydroxylation reactions are oxygen dependent, decreases in oxygen concentration (hypoxia) result in (i) disruption of VHL binding to and degradation of HIF, leading to accumulation of HIF levels, and (ii) promotion of p300 binding, leading to an increase in HIF transcriptional activity.

Although the exact mechanism is under debate, the oxygen-dependent effects of FIH on HIF activity suggest that it acts as a cellular "oxygen sensor" that is important in the transduction of environmental hypoxic cues into appropriate cellular signals such as HIF-mediated upregulation of glycolytic and angiogenic genes (32, 37). Nevertheless, the list of bona fide hydroxylation targets of FIH is limited. In the present report, we demonstrate that ASB4 is expressed during vascular development in a window of time during which oxygen tensions are rapidly changing, is a direct target for FIH-dependent hydroxylation, and promotes differentiation into the vascular lineage in an oxygen-dependent manner.

MATERIALS AND METHODS

Plasmids. Flag-tagged mouse ASB4 in pEF1 and Flag-tagged mouse ASB1 in pEF1 were generous gifts from W. Alexander. All PCR amplimers for cloning were TA cloned, sequenced for accuracy, and (unless otherwise noted) subcloned into destination vectors as N-terminally tagged mouse sequences. All amino acid locations refer to accession no. NP_075535. For the constructs used, along with the destination vectors and primer pairs, see Table S1 in the supplemental material. Internal deletion mutants and point mutants were generated with the QuikChange mutagenesis system (Stratagene) with Flag-ASB4 in pCMV as the template; for the primers used, see Table S1 in the supplemental material (since primers are reverse complements of each other, only one primer per pair is listed). pGBKT7, pGADT7, pGBKT7-p53, and pGADT7-T were from Clontech. To generate Flag-ASB4- and Flag-ASB4ΔSOCS-encoding adenoviruses, PCR-produced, Xba-flanked inserts were subcloned into the XbaI site of pAdTrack-CMV. All adenoviruses coexpressed cytomegalovirus promoter-driven green fluorescent protein (GFP).

Antibodies. Antibodies against FIH (NB 100-428; Novus), Flag (F1804; Sigma), myc (sc-789; Santa Cruz), Cul2 (gift from Y. Xiong) (36), Cul5 (gift from Y. Xiong; raised against the peptide SNLLKNKGSLQFEDK), elongin B (sc-1558; Santa Cruz), Roc1 (gift from Y. Xiong) (36), and ubiquitin (MMS-258R; Covance) were used for immunoblotting. Flag-agarose beads (A2220; Sigma) and myc-agarose beads (sc-40 ac; Santa Cruz) were used for immunoprecipitation.

Cell culture and transfection conditions. Embryonic stem (ES) cell culture, differentiation, and fluorescence-activated cell sorter (FACS) analysis have been described previously (34). Normoxic cultures were performed under atmospheric oxygen tension (~21%) and 5% CO_2. Hypoxia culture was at 1% O_2 and 5% CO_2. HEK-293T cells were used in all transfection experiments with Fugene 6 reagent (Roche). RNA interference (RNAi) experiments used Dharmafect I (Dharmacon) and prevalidated small interfering RNA (siRNA) duplexes. Cells were incubated for 24 h before lysis. For generation of ASB4 stable ES cells, 3×Flag-ASB4 in p3xflag-CMV10 (Sigma) was linearized and electroporated into R1 ES cells, which were selected with 250 μg/ml G418 for 14 days. Selective clones were picked, amplified, and confirmed by anti-Flag immunoblotting. COS7 cells were used for adenoviral infection.

Microarray analysis. Purification and amplification of total RNA from ES cells, reverse transcription, and microarray techniques have been described previously (46). For this analysis, the data set was subjected to supervised hierarchical clustering with only genes demonstrating a ≥1.5-fold absolute mean difference in 84-h $Flk1^+$ cells from embryoid bodies. Median centered genes and arrays were clustered with Cluster (version 2.11; http://rana.lbl.gov/EisenSoftware.htm), and heat maps of cluster analyses were visualized with JavaTreeView (version 1.0.12; release date, 14 March 2005; http://sourceforge.net/projects/jtreeview/).

Reverse transcriptase PCR (RT-PCR) analysis. Total RNA was isolated with the RNeasy system (QIAGEN). RNA was reverse transcribed with SuperScript II RT (Invitrogen) using the following oligo(dT) primers: ASB4 PCR, forward primer 5′GAGACACCCCTGCACACGGCAG and reverse primer 5′CTCAG GCTGTGCAGCAGGACGC; glyceraldehyde-3-phosphate dehydrogenase (GAPDH), forward primer 5′ACCACAGTCCATGCCATCAC and reverse primer 5′TCC ACCACCCTGTTGCTGTA.

For real-time PCR analysis, total RNA was reverse transcribed with the iScript system (Bio-Rad) and a mixture of oligo(dT) and random hexamer primers. Real-time PCRs were performed with the ABI PRISM 7900 sequence detection system, software, and reagents. The following prevalidated primer and probe sets based on Taqman chemistry (Applied Biosystems) were used: Flk1 (accession no. mM01222419_m1), PECAM (accession no. mM00476702_m1), VE-cadherin (accession no. mM00486938_m1), Tie2 (accession no. mM01256892_m1), Gata1 (accession no. mM00484678_m1), Klf1 (accession no. mM00516096_m1), Scl/Tal (mM00441665_m1), and brachyury (accession no. mM00436877_m1). Triplicate reaction mixtures with independent RNA samples were prepared. RNA input was calibrated with 18S expression levels, and relative mRNA levels were normalized to levels from empty-vector-transfected, undifferentiated ES cells.

Whole-mount in situ hybridization. Whole-mount in situ hybridization on mouse embryos has been previously described (34). A 900-bp template for ASB4 probe preparation was prepared with forward primer 5′TATCCATGGTGGAC GGCATCACTGCCCCTATC and reverse primer 5′CTCAGGCTGTGCAGCA GGACGC) and TA cloned into the pCRIItopo vector (Invitrogen). Digoxigenin-labeled single-strand sense and antisense RNA probes were prepared with the digoxigenin (DIG) RNA labeling system (Roche).

RNA isolation and Northern blot analysis. Tissues of CD1 embryos and C57BL/6 adult mice were homogenized and used to prepare total RNA (RNeasy system; QIAGEN). Northern blot analysis has been described previously (34). A 400-bp ASB4 probe was amplified with forward primers 5′GAGACACCCCTG CACACGGCAG and reverse primer 5′CTCAGGCTGTGCAGCAGGACGC, TA cloned into vector pCR2.1 (Invitrogen), digested with EcoRI, gel purified, and used as the template for radioactive double-stranded random-primed probe synthesis (Stratagene).

Immunoprecipitation and immunoblot analysis. Immunoprecipitation and immunoblotting procedures have been described previously (28). Unless otherwise noted, cells were lysed in buffer (50 mM Tris-HCl [pH 7.4], 150 mM NaCl, 1% Triton X-100, 1× Complete protease inhibitor cocktail [Roche]). One milligram of protein lysate was incubated with 30 μl of Flag- or myc-conjugated beads overnight at 4°C. Beads were washed four times with a >20× volume of lysis buffer, boiled in 30 μl of 2× sodium dodecyl sulfate loading buffer containing β-mercaptoethanol for 5 min, and loaded onto 10% protein gels. After electrophoresis, gels were transferred to polyvinylidene difluoride membranes and immunoblotted.

Yeast two-hybrid assay. Yeast two-hybrid screens for ASB4 binding partners were performed with Matchmaker 2-Hybrid system 2 (Clontech) as previously described (28). ASB4ΔSOCS/GAL4 DNA-binding domain in vector pGBKT7 was transformed into AH109 yeast cells as bait, mated with pretransformed cDNA library-containing Y187 yeast (HY4042AH; Clontech), and spread onto agar plates lacking Trp, Leu, His, and Ade for high-stringency selection. To reconfirm interactions, both ASB4ΔSOCS in pGBKT7 and prey constructs were cotransfected in various combinations with empty vectors (EVs) as negative controls and pGBKT7-p53/pGADT7-T vectors as a positive interaction control.

Molecular model development. A fragment of mouse ASB4 spanning AR6 and -7 (V^{201} through A^{288}) was used to query various fold recognition servers, including FUGUE (http://tardis.nibio.go.jp/fugue/prfsearch.html), INUB (http://inub.cse.buffalo.edu/), and PHYRE (http://www.sbg.bio.ic.ac.uk/phyre/). Several AR-containing protein crystal structures were identified as possessing folds similar to the mouse ASB4 fragment query. Homologous regions of three crystal structures were used as templates for model prediction, (i) PYK2-associated protein beta (PDB accession no. 1DCQ), (ii) Bcl-3 (PDB accession no. 1K1A), and (iii) the *Drosophila* Notch receptor (PDB accession no. 1OT8). Models of the ASB4 ARs were built, guided by the alignments returned from the fold recognition servers, with the Modeler module of the InsightII molecular modeling system from Accelrys Inc. (www.accelrys.com).

Mass spectrometry (MS). Immunoprecipitates of Flag-ASB4-infected COS7 cells were loaded onto protein gels and stained with Coomassie brilliant blue, and the bands of interest were cut and processed according to the previously published protocols from the University of North Carolina-Duke Michael

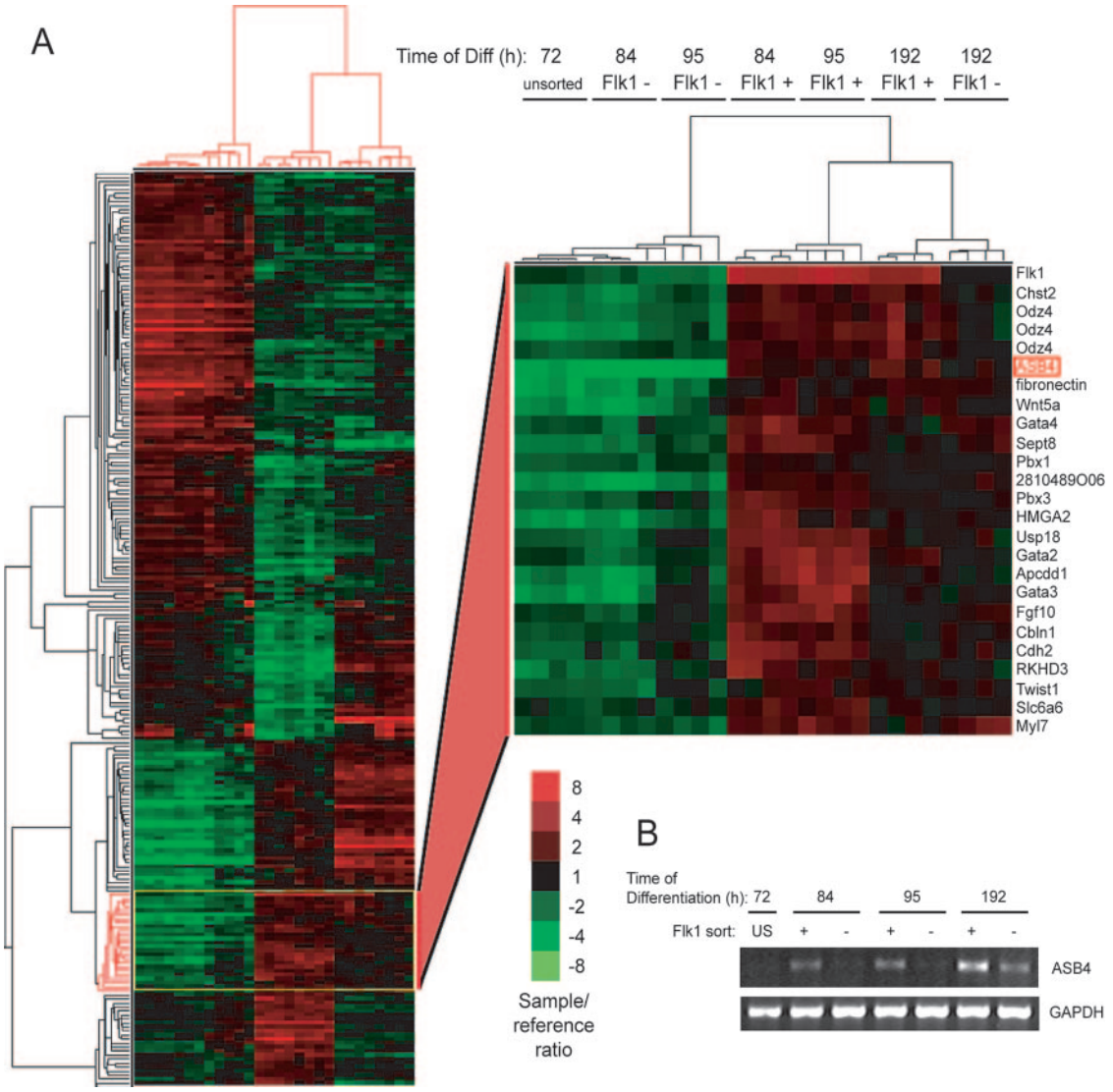

FIG. 1. ASB4 is highly differentially expressed in the vascular lineage during ES cell differentiation (Diff). (A) Supervised hierarchical cluster of genes with a ≥1.5-fold absolute mean difference in 84-h Flk1$^+$ cells from embryoid bodies. The Flk1 cluster containing ASB4 is shown at the right. This experiment was described in detail by Wang et al. (46), and the complete data set is available online through the Gene Expression Omnibus (series record GSE3757, http://www.ncbi.nlm.nih.gov/geo) and through the University of North Carolina Microarray Database (http://genome.unc.edu). Experiments were performed in quadruplicate. (B) RT-PCR analysis of ASB4 expression levels in Flk1$^+$ cells from differentiated embryoid bodies. GAPDH was used as a loading control. US, unsorted.

Hooker Proteomics Center (38). Peptide digests were analyzed on an ABI 4700 proteomic analyzer by matrix-assisted laser desorption ionization–time of flight (MALDI-TOF; Applied Biosystems, Inc., Foster City, CA), and the identity of the protein was confirmed by searching the MS results as outlined previously (38). Following protein identification, the peptide mixtures were respotted and the peptide (*m*/*z* 1,345.67) corresponding to the hydroxylated ASB4 peptide (*m*/*z* 1,329.68) was analyzed by tandem MS (MS/MS) along with the unhydroxylated peptide. For determination of peptide peak ratios, the curve areas of the *m*/*z* 1,329.68 and *m*/*z* 1,345.66 peptide peaks, relative to the curve area of the *m*/*z* 1,512.823 peptide peak (shown by MS/MS in all samples to be derived from ASB4), were determined.

RESULTS

ASB4 is expressed in the vascular lineage of differentiating ES cells. In order to identify genes important during vascular development, we performed a set of experiments that compared the gene expression profiles of Flk1$^+$ and Flk1$^-$ cells isolated during different stages of differentiating ES cells (described by Wang et al. [46]). Out of 20,000 genes, ASB4 was the most highly differentially expressed gene in Flk1$^+$ cells, compared to Flk1$^-$ cells, at early time points of differentiation (Fig. 1A). This differential expression was confirmed by RT-PCR analysis showing that ASB4 mRNA is highly enriched in the Flk1$^+$ population at 84 h, 95 h, and 192 h of differentiation but is undetectable at 72 h of differentiation (before Flk1 is expressed in this system) (Fig. 1B). Since Flk1 is expressed in early precursor cells of the endothelial, hematopoietic, vascular smooth muscle, and cardiomyocyte lineages (20), we reasoned that ASB4 could be important during cardio- and/or hematovascular development. In support of this, supervised

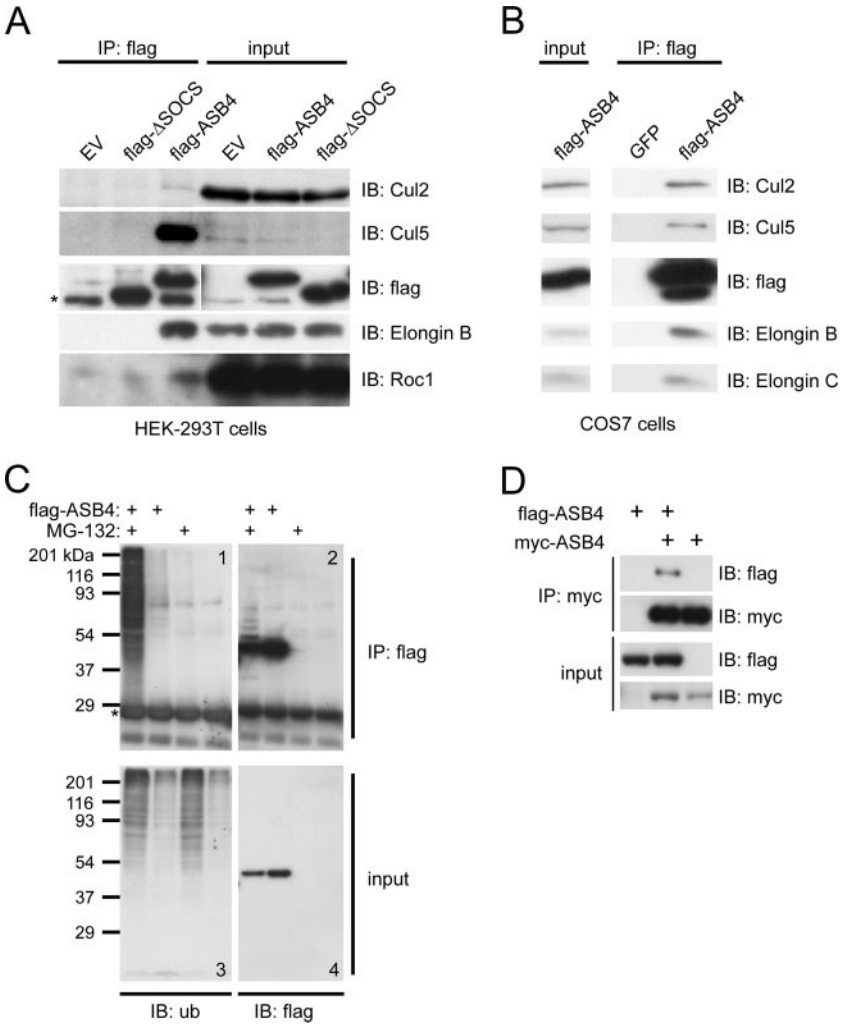

FIG. 2. ASB4 associates with a ubiquitin ligase complex. (A) HEK-293T cells were transfected with Flag-ASB4, Flag-ASB4ΔSOCS (flag-ΔSOCS), or the EV pCMV. Lysates were immunoprecipitated (IP) with anti-Flag–agarose beads and subjected to immunoblotting (IB) with anti-Flag, -Cul2, -Cul5, -elongin B, and -Roc1 antibodies. Asterisks denote nonspecific bands. (B) COS7 cells were infected with Flag-ASB4 adenovirus or GFP-alone adenovirus (GFP). Lysates were immunoprecipitated and immunoblotted as described for panel A. (C) HEK-293T cells were transfected with Flag-ASB4, cultured for 20 h, and then treated with the proteasome inhibitor MG-132 at 40 μM for 4 h before protein harvesting. Lysates were immunoprecipitated as described for panel A and immunoblotted with antiubiquitin (ub) and anti-Flag antibodies. (D) HEK-293T cells were cotransfected with Flag-ASB4 and myc-ASB4, immunoprecipitated with anti-myc agarose beads, and immunoblotted.

hierarchical clustering analysis with only genes demonstrating a ≥1.5-fold absolute mean fold difference in 84-h Flk1$^+$ cells showed that ASB4 clusters closely with other genes known to be important in cardiovascular development, including Flk1, fibronectin, Gata2, and Gata4 (Fig. 1A).

The SOCS box-containing protein ASB4 assembles with a ubiquitin ligase complex. Since other SOCS box-containing proteins function as substrate adaptor proteins for elongin B/elongin C/cullin/Roc ubiquitin ligase complexes by binding the complex in a SOCS box-dependent manner, we investigated whether ASB4 exists in such complexes and can function as a ubiquitin ligase. In transient transfection assays with HEK-293T cells, Flag-ASB4, but not the EV or a mutant lacking the C-terminal SOCS box (ΔSOCS), coprecipitated endogenous elongin B, Cul5, Roc1, and to a lesser extent Cul2 (Fig. 2A). The signal for coprecipitation of Cul2 was greatly increased with lysates from COS7 cells infected with Flag-ASB4 adenovirus (Fig. 2B), indicating that ASB4 can use Cul2 or Cul5 complexes and that this preference is dependent upon the cellular context. Given that other ASBs associate with Cul5/Roc1 and Cul5/Roc2 complexes, further studies are needed to determine if the Cul2 interaction is unique to ASB4 or inherent to all ASBs in the appropriate context and if ASB4 function is affected by the cullin complex used. Notably, VHL associates with Cul2, suggesting that ASB4 may share molecular mechanisms with VHL (5, 12, 18, 23).

To evaluate whether ASB4 functions as part of a ubiquitin ligase complex, in vivo ubiquitination assays were performed. HEK-293T cells were transfected with Flag-ASB4 for 20 h, followed by treatment with the proteasome inhibitor MG-132 to allow polyubiquitin-tagged protein accumulation. Flag-tagged immunoprecipitates were then immunoblotted with anti-Flag and antiubiquitin antibodies. Strong ubiquitin immunoreactivity was detected in Flag-tagged immunoprecipitates

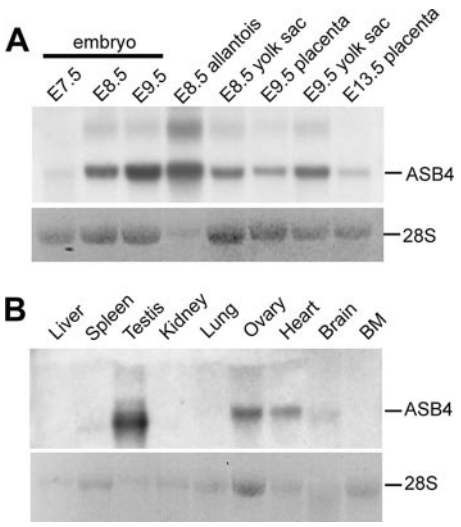

FIG. 3. ASB4 mRNA expression in embryonic and adult tissues. (A) Northern blot analysis of ASB4 expression levels in whole embryos and dissected extraembryonic tissues. (B) Northern blot analysis of ASB4 expression levels in adult tissues. BM, bone marrow. Ethidium bromide staining of 28S rRNA was used as a loading control.

of Flag-ASB4-transfected cells after MG-132 treatment (Fig. 2C, part 1). We reasoned that this signal could represent ubiquitinated ASB4-associated proteins, ubiquitinated ASB4 itself, or both. A 7-kDa Flag-tagged immunoreactive laddering pattern was detected in Flag-tagged immunoprecipitates after treatment with MG-132, indicating that ASB4 itself is ubiquitinated (Fig. 2C, part 2). Furthermore, Flag-ASB4 coprecipitates with myc-ASB4 in cotransfected HEK-293T cells, indicating that ASB4 complexes with itself (Fig. 2D). Since additional coimmunoprecipitation experiments with HEK-293T cells did not indicate that substrates are stably associated with ASB4 in this cell type (data not shown), these data indicate that ASB4 is most likely autoubiquitinated (which may represent a mechanism of self-regulation) and thus behaves like a ubiquitin ligase in this system.

ASB4 is expressed in the embryonic vasculature during a narrow time window. To determine that ASB4 expression is high in anatomic locations known to harbor active vascular development and remodeling and to further define exactly which tissue(s) ASB4 expression is confined to, we analyzed its expression in embryonic and adult tissues. Global ASB4 mRNA expression is comparatively low in E7.5 embryos but quickly increases until E9.5 (Fig. 3A). Highly vasculogenic tissues such as the allantois, yolk sac, and placenta all express high levels of ASB4. However, while ASB4 expression in the adult is highest in the testis, ovary, and heart, it is undetectable in highly vascular organs such as the lung, kidney, and liver (Fig. 3B), suggesting that ASB4 function may be critical to proper vascular development but dispensable for the maintenance of adult vessels in some tissues. Furthermore, tissues containing high numbers of hematopoietic cells such as those of the spleen and bone marrow have undetectable levels of ASB4 mRNA expression.

To further define the anatomic location of ASB4 expression during embryogenesis, we performed whole-mount in situ hybridization analysis with DIG-labeled ASB4 antisense riboprobes on mouse embryos at various gestational stages. In E9.5 embryos, ASB4 is expressed in the intersomitic vessels, dorsal aorta, forelimb buds, allantois/umbilical vessels, vitelline vessels, septum transversum, proepicardium, capillary plexi of the head and branchial arches, endocardium, and yolk sac vasculature (Fig. 4A, B, D, G, and H). In E10.5 embryos, areas with high ASB4 expression levels include the forelimb and hind limb buds, intersomitic vessels, peripheral liver cells, and umbilical vessels (Fig. 4E and I). In E11.5 embryos, high levels of ASB4 expression are limited to the forelimbs and hind limbs and the most caudal (and most recently formed) intersomitic vessels (Fig. 4F). Notably, E7.5 embryos show no remarkable ASB4 staining (data not shown). Analysis with sense probes confirmed the specificity of the antisense signal (Fig. 4C).

The most striking recurring pattern of ASB4 embryonic expression is its high levels in primitive capillary plexi, followed by downregulation as vessels mature. At E9.5, ASB4 is highly expressed in the capillary plexi of the head and branchial arches (Fig. 4B), but by E10.5 expression in these vascular beds is no longer detectable (Fig. 4E). Similarly, ASB4 expression is high in intersomitic vessels at E10.5 but by E11.5 is confined to only the most caudal (and thus recently formed) intersomitic vessels (Fig. 4F). This pattern is recapitulated in the placenta, with high ASB4 expression in the immature placenta at E9.5 compared to the mature placenta at E13.5 (Fig. 3A). Finally, ASB4 expression is undetectable in highly vascularized adult organs such as the kidney and lung (Fig. 3B). This dynamic temporal regulation of ASB4 expression suggests that its function is temporally limited. Notably, the endothelium is exposed to drastic increases in oxygen tension between E9.5 and E10.5 as the placenta develops and maternal-fetal blood gas exchange is initiated. Since another SOCS box-containing protein, VHL, is known to regulate the cellular response to changing oxygen concentrations and since ASB4 may share molecular mechanisms with VHL, we postulated that ASB4 may function during development in an oxygen-dependent manner to modulate an endothelium-specific oxygen response during a time at which oxygen tension drastically increases.

ASB4 binds to FIH by using a conserved motif. As a first step in the mechanistic characterization of ASB4, we attempted to identify ASB4 binding partners with the yeast two-hybrid system. We used an ASB4 mutant lacking the C-terminal SOCS box (ASB4ΔSOCS) as bait to avoid reconfirmation of interactions with known SOCS box binding partners elongin B and elongin C. With a human heart oligo(dT)-primed pretransformed yeast library, we screened more than 1.5×10^7 independent clones and identified FIH as an interacting protein under stringent conditions (positive clones grew on plates lacking tryptophan, leucine, histidine, and adenine). The FIH prey clone encoded all but the five most N-terminal amino acids of the human FIH protein. This interaction was confirmed in a wheel assay in which yeast cells were transformed with various combinations of ASB4ΔSOCS bait, FIH prey, EVs (V1, V2), or mismatched nonspecific controls (Fig. 5A). p53- and T-antigen (T)-containing plasmids were used as positive controls for an interaction in this system. Flag-tagged immunoprecipitates of HEK-293T cells overexpressing Flag-ASB4 but not Flag-ASB1 coimmunoprecipitated endogenous

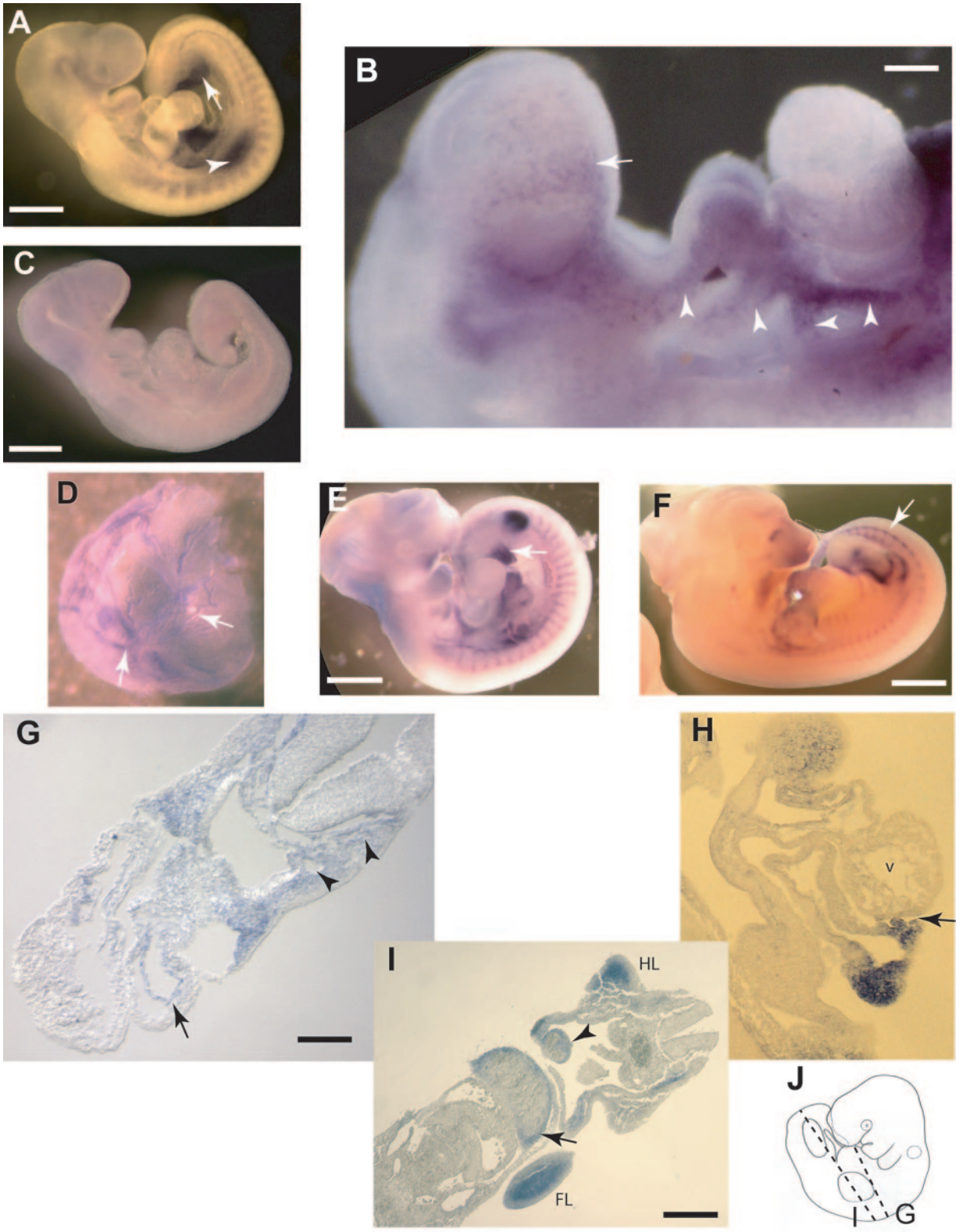

FIG. 4. Localization of ASB4 mRNA during mouse embryogenesis. Whole-mount in situ hybridization with DIG-labeled RNA probes for ASB4 was performed on E9.5 to E11.5 mouse embryos. (A) E9.5 embryo. Arrow, allantois; arrowhead, forelimb; bar, 500 μm. (B) E9.5 embryo at high magnification. Arrow, rostral capillary plexus; arrowheads, branchial arch capillary plexi; bar, 50 μm. (C) E9.5 embryo probed with sense probe as a negative control. Bar, 500 μm. (D) E9.5 yolk sac. Arrows, yolk sac vessels; bar, 750 μm. (E) E10.5 embryo. Arrow, umbilical vessels; bar, 800 μm. (F) E11.5 embryo. Arrow, caudal intersomitic vessels; bar, 1 mm. (G) Transverse section of E9.5 embryo heart. Arrow, endocardium; arrowheads, dorsal aorta and intersomitic vessel; bar, 80 μm. (H) Sagittal section of E9.5 embryo heart. v, ventricle; arrow, pro-epicardium/septum transversum. (I) Transverse section of E10.5 embryo liver. HL, hind limb; FL, forelimb; arrow, liver; arrowhead, umbilical vessels; bar, 150 μm. (J) Schematic of section location in panels G and I. Antisense probes were used for all images except that in panel C (sense probe). Purple staining denotes a positive signal. In some cases (G, H, and I), stained whole embryos were paraffin embedded and sectioned for microscopic examination.

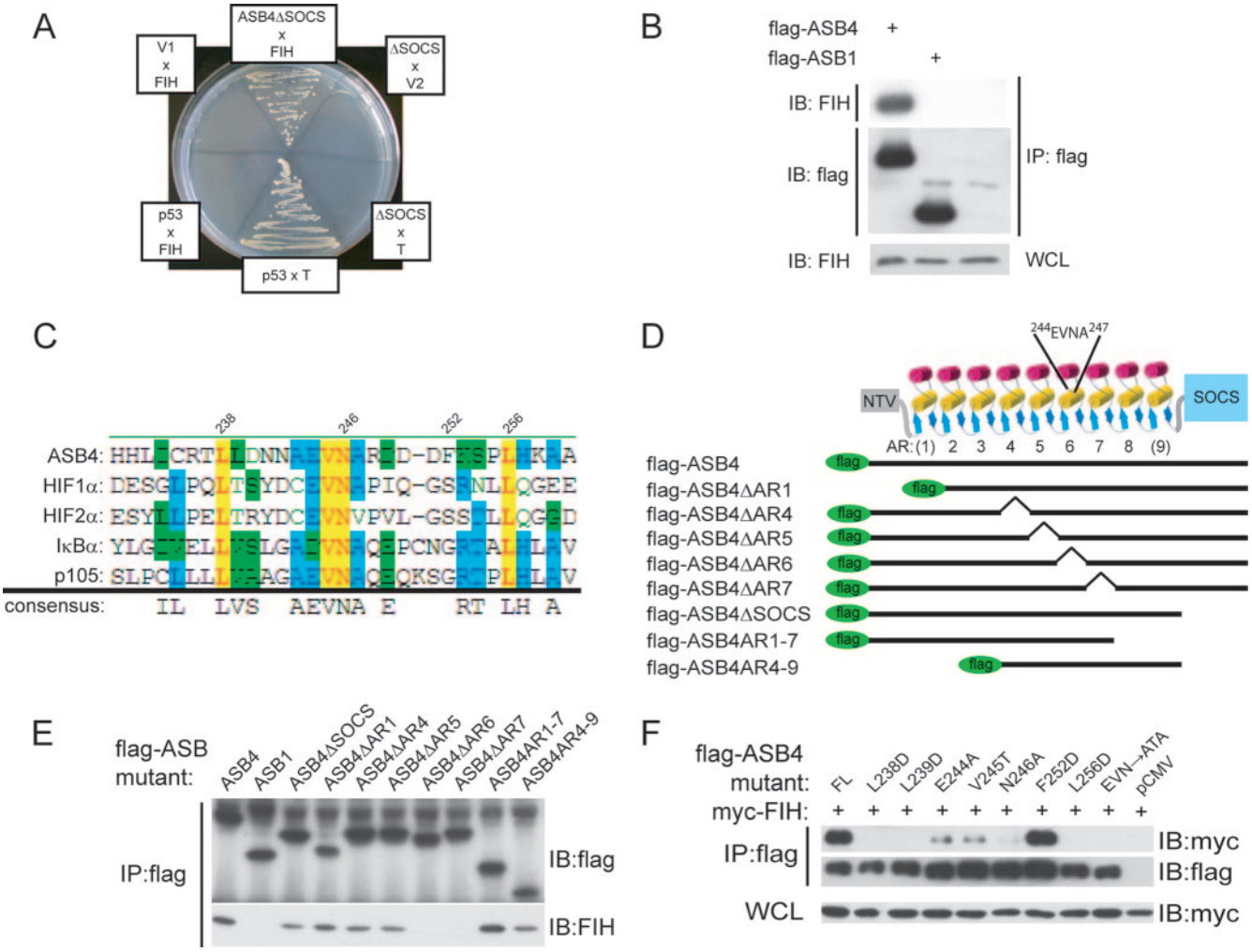

FIG. 5. ASB4 binds to FIH through a conserved motif in AR6. (A) Yeast wheel assay. Yeast cells transformed with different combinations of bait (ASB4ΔSOCS) and prey (FIH) constructs were spread onto a high-stringency selective plate lacking tryptophan, leucine, histidine, and adenine. p53 and T were used as positive controls. V1, empty bait vector (pGBKT7). V2, empty prey vector (pGADT7). (B) HEK-293T cells were transfected with either Flag-ASB4 or Flag-ASB1. Lysates were immunoprecipitated (IP) with Flag antibody-conjugated agarose beads and immunoblotted (IB) with anti-Flag and anti-FIH antibodies. (C) Sequence alignment of mouse ASB4 and other known FIH hydroxylation substrates. The consensus sequence shows high conservation of E244, V245, N246, A247, and flanking leucine residues. Residue numbers are indicated above the ASB4 sequence. (D) Schematic of ASB4 with the N-terminal variable region (NTV), nine tandem ARs (poorly conserved repeats are indicated by parentheses), and a C-terminal SOCS box. Asparagine 246 is contained in the loop of AR6. Schematics of N-terminally Flag-tagged constructs are denoted below. (E) HEK-293T cells were transfected with Flag-ASB4, Flag-ASB1, and the Flag-ASB4 deletion mutants described in panel D. Protein lysates were immunoprecipitated with anti-Flag–agarose and immunoblotted with anti-FIH antibody. (F) HEK-293T cells were transfected with various Flag-ASB4 point mutants and myc-FIH. Lysates were immunoprecipitated with Flag antibody-conjugated agarose beads and immunoblotted with anti-Flag and anti-myc antibodies. WCL, whole-cell lysate.

FIH, confirming the specificity of this interaction in mammalian cells (Fig. 5B).

FIH is an asparagine hydroxylase that is known to hydroxylate at least four proteins, HIF1α, HIF2α (27) IκBα, and the NF-κB precursor protein p105 (3). Since the hydroxyl group is derived directly from atmospheric dioxygen, this reaction is oxygen dependent and thus FIH is often referred to as a cellular "oxygen sensor." This raised the intriguing possibility that ASB4 is a hydroxylation substrate of FIH and may therefore be regulated by atmospheric oxygen tension. FIH has been shown to bind to and hydroxylate its substrates on the β carbon of a leucine-flanked asparagine residue within ARs (3). The flanking leucines bind first to position the asparagine for optimal binding in the FIH catalytic cleft via a process called "induced fit" (7). Sequence alignment of ASB4 with four other known FIH substrates revealed a conserved leucine-flanked asparagine in AR6 (Fig. 5C). This alignment also indicates highly conserved residues surrounding the asparagine, including perfect conservation of Val 245. Notably, all of these residues (leucines, valine, and asparagine) have previously been shown to be involved in FIH-substrate interactions (29). To test whether AR6 is necessary for interaction with FIH, a variety of N-terminally Flag-tagged mutants were generated that sequentially lack different domains of the ASB4 protein (Fig. 5D). Since the hydrophobic interactions between helices of adjacent ARs are crucial for proper folding, we carefully

positioned the borders of the deletions in order to best conserve the modular structure of the mutants. These mutants were transiently transfected into HEK-293T cells, Flag immunoprecipitated, and immunoblotted with anti-FIH antibody to detect coprecipitating endogenous FIH protein (Fig. 5E). ASB4 AR6 and -7 are necessary for interaction with FIH since mutants lacking either AR6 or -7 were unable to coprecipitate FIH. Mutants lacking other ARs (AR1, -4, -5, or -8, -9) or the SOCS box were still able to coprecipitate FIH, indicating that these domains are dispensable for FIH binding and that deletion of single ARs does not disrupt the tertiary structure of the FIH-interacting motif.

To test the involvement of the leucine-flanked asparagine and surrounding residues in FIH binding, we generated a number of point mutants in and around this motif to test their involvement in the FIH interaction. Each Flag-tagged point mutant was transiently transfected with N-terminal myc-FIH, immunoprecipitated with anti-Flag-conjugated agarose beads, and immunoblotted with anti-myc antibody to detect coprecipitating myc-FIH. Consistent with the "induced fit" model, point mutation of any of the flanking leucines to aspartate residues (L238D, L239D, and L256D) reduced coprecipitating myc-FIH to undetectable levels (Fig. 5F). Single-point mutation of the asparagine residue (N246A) reduced binding to undetectable levels, while mutation of the adjacent glutamate (E244A) or valine (V245T) residue reduced but did not abolish binding. Mutation of the EVN residues to ATA abolished binding to undetectable levels. Taken together, these data indicate that ASB4 binds to FIH through a conserved hydroxylation motif in AR6 and suggest that ASB4 may be a novel FIH hydroxylation substrate.

We also tested the alternative hypothesis that ASB4 inhibits FIH activity either by ubiquitin-mediated proteasomal degradation or by enzymatic blockade via a competitive binding mechanism. We found that ASB4 has no effect on FIH ubiquitination and that overexpression of ASB4 does not result in the activation of HIF-responsive luciferase reporter genes or in the upregulation of multiple HIF target genes in endothelial cell lines (data not shown).

ASB4 is hydroxylated on asparagine 246 by an oxygen-dependent mechanism. To determine if the leucine-flanked asparagine is positioned in an appropriate conformation to allow binding to and hydroxylation by FIH, we generated a structural model of ASB4 AR6 and -7 (Fig. 6A). This model shows that the asparagine and flanking leucine residues of ASB4 are optimally positioned to allow an induced fit of the asparagine into the catalytic cleft of FIH and prompted further studies to examine the possibility of FIH-mediated ASB4 hydroxylation.

To test the hypothesis that ASB4 is an FIH hydroxylation substrate, adenovirus-overexpressed Flag-ASB4 was Flag immunoprecipitated from COS7 cells grown under normoxic culture conditions, in-gel trypsinized, and analyzed by MALDI-TOF MS. The predicted mass/charge ratio (*m*/*z*) of the Asn 246-containing trypsin-digested peptide TLLDNNAEVNAR is 1,329, and hydroxylation of this peptide will result in a 16-Da shift to 1,345. By MALDI-TOF analysis, we detected the 1,329-Da peptide and a 1,345-Da peptide that did not match the predicted *m*/*z* value for any of the peptides from trypsin-digested Flag-ASB4, suggesting that the *m*/*z* 1,345 peak represents the hydroxylated form of the 1,329-Da peptide (Fig. 6B). This was confirmed through MALDI-TOF-TOF MS/MS sequencing analysis of the 1,329- and 1,345-Da peptides, separately. Alignment of the MS/MS spectra of the 1,329- and 1,345-Da peptides demonstrates that the 16-Da shift due to hydroxylation is present only in peptide ions containing Asn 246, indicative of FIH-mediated asparagine hydroxylation of ASB4 (Fig. 6C).

Under normoxic conditions (21% oxygen), the ratio of unhydroxylated to hydroxylated ASB4 peptide is 3.1:1, indicating that under normoxic conditions, only ~25% of ASB4 is hydroxylated (Fig. 6D). To test if this was due to saturation of endogenous FIH enzymatic activity by supraphysiologic concentrations of transfected ASB4, we coexpressed ASB4 and FIH in HEK-293T cells, which resulted in the hydroxylation of nearly all (89%) of the ASB4. These results emphasize the importance of the stoichiometric ratio of FIH and its substrates for hydroxylation activity, and further studies that evaluate what percentage of endogenous ASB4 is hydroxylated are needed. To confirm that ASB4 hydroxylation was indeed dependent on endogenous FIH, we cotransfected cells with siRNA duplexes against either FIH or GAPDH as a negative control. Immunoblot analysis confirmed the successful knockdown of FIH, and the percentage of hydroxylated ASB4 in cells lacking FIH (7%) was threefold less than that in the negative controls (21%). Since FIH-mediated hydroxylation of known substrates is O_2 dependent (and thus inhibited by hypoxia), we tested whether hypoxic conditions would decrease ASB4 hydroxylation. Importantly, when HEK-293T cells transfected with Flag-ASB4 were cultured under hypoxic conditions (1% oxygen), the percentage of hydroxylated ASB4 peptide dropped to 7%. Similar results were obtained when these cells were treated with chemical hypoxia mimetics ($CoCl_2$ and dipyridyl) or hydroxylase inhibitors (dimethyloxalylglycine) (data not shown). Together, these data demonstrate that FIH hydroxylates ASB4 at Asn 246 via an oxygen-dependent mechanism and suggest that ASB4 function may be regulated by oxygen concentrations.

We next tested whether ASB4 hydroxylation affects ASB4 stability or autoubiquitination by repeating the in vivo ubiquitination experiments described in Fig. 2 with unhydroxylatable mutants (ΔAR6 and EVN→ATA) or coexpression of FIH. Steady-state levels of ASB4 and levels of autoubiquitination were not affected by these parameters (data not shown).

ASB4 functions to promote ES cell differentiation into the vascular lineage in an oxygen-dependent manner. Since we were unable to identify any effects of ASB4 over- or underexpression in multiple cell lines (data not shown) and since other SOCS family proteins are known to regulate cell differentiation, we investigated the effects of ASB4 overexpression on ES cell differentiation into the vascular lineage and whether these effects can be regulated by oxygen concentration.

First, to determine the effects of ASB4 overexpression on this system, mouse ES cells were electroporated with linearized 3×Flag-tagged ASB4, the unhydroxylatable ASB4 ΔAR6 and EVN→ATA mutants, or the p3Xflag-CMV EV and placed in G418 to select for stable transfected clones. (We also attempted RNAi-mediated knockdown of ASB4 with six different short hairpin RNA sequences from integrated lentivirus constructs but were unable to attain greater than 40% silencing [data not shown], indicating that the ASB4 transcript may be

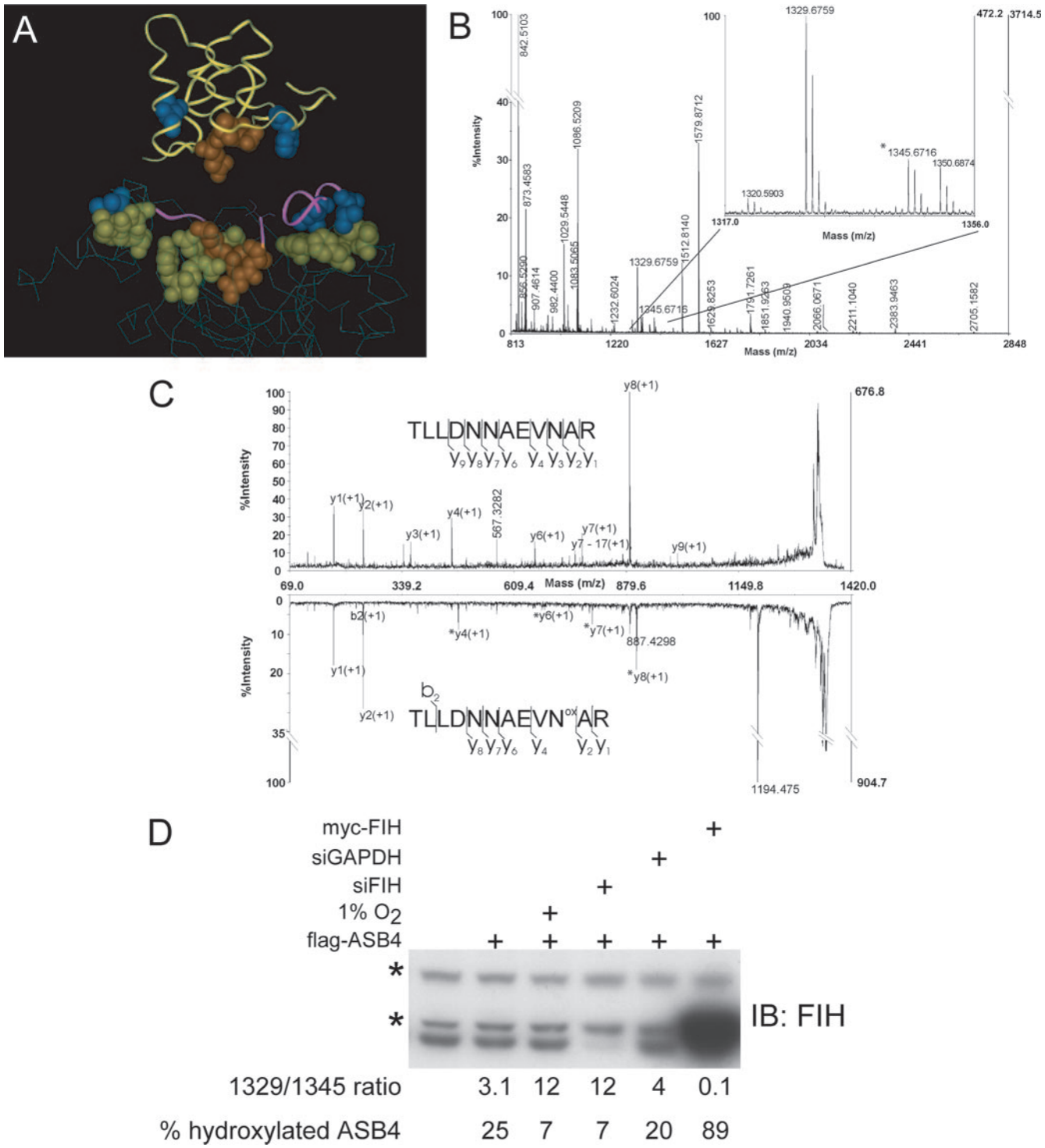

FIG. 6. ASB4 is hydroxylated on asparagine 246 by an oxygen-dependent mechanism. (A) Structural model of ASB4 AR6 and -7 (yellow ribbon backbone) positioned above the FIH (gray stick backbone)/HIF peptide (purple ribbon backbone) crystal structure (PDB accession no. 1H2K). Space-filled EVNA residues are colored orange. Space-filled FIH residues contributing to HIF binding are colored yellow. Leucines and other possible hydrophobic interacting residues are colored blue. (B) COS7 cells were infected with Flag-ASB4 adenovirus for 24 h. Lysates were immunoprecipitated with Flag antibody-conjugated agarose beads. Beads were eluted with Flag-tagged peptide and subjected to sodium dodecyl sulfate-polyacrylamide gel electrophoresis and Coomassie staining. Flag-ASB4 bands were subjected to in-gel trypsin digestion and MALDI-TOF MS analysis. The 1,329-Da peak represents the unhydroxylated form of the asparagine-containing peptide, and the 1,345-Da peak (asterisk) represents the hydroxylated form of the peptide. (C) The 1,329- and 1,345-Da peptides were analyzed by MS/MS. A 16-Da shift was observed with the y4-y8 ions but not with the y2 ions, consistent with hydroxylation at the asparagine residue. (D) HEK-293T cells transiently transfected with Flag-ASB4 were cotransfected with myc-FIH or siRNA targeting FIH or GAPDH (negative control) or cultured under hypoxic conditions (1%). Flag-ASB4 protein was isolated and analyzed as for panel B, and the peak area ratio of unhydroxylated (1,329 Da) to hydroxylated (1,345 Da) peptide was calculated to evaluate the percentage of hydroxylated ASB4. In parallel, whole-cell lysates were subjected to immunoblotting (IB) by FIH antibody. Asterisks indicate nonspecific bands.

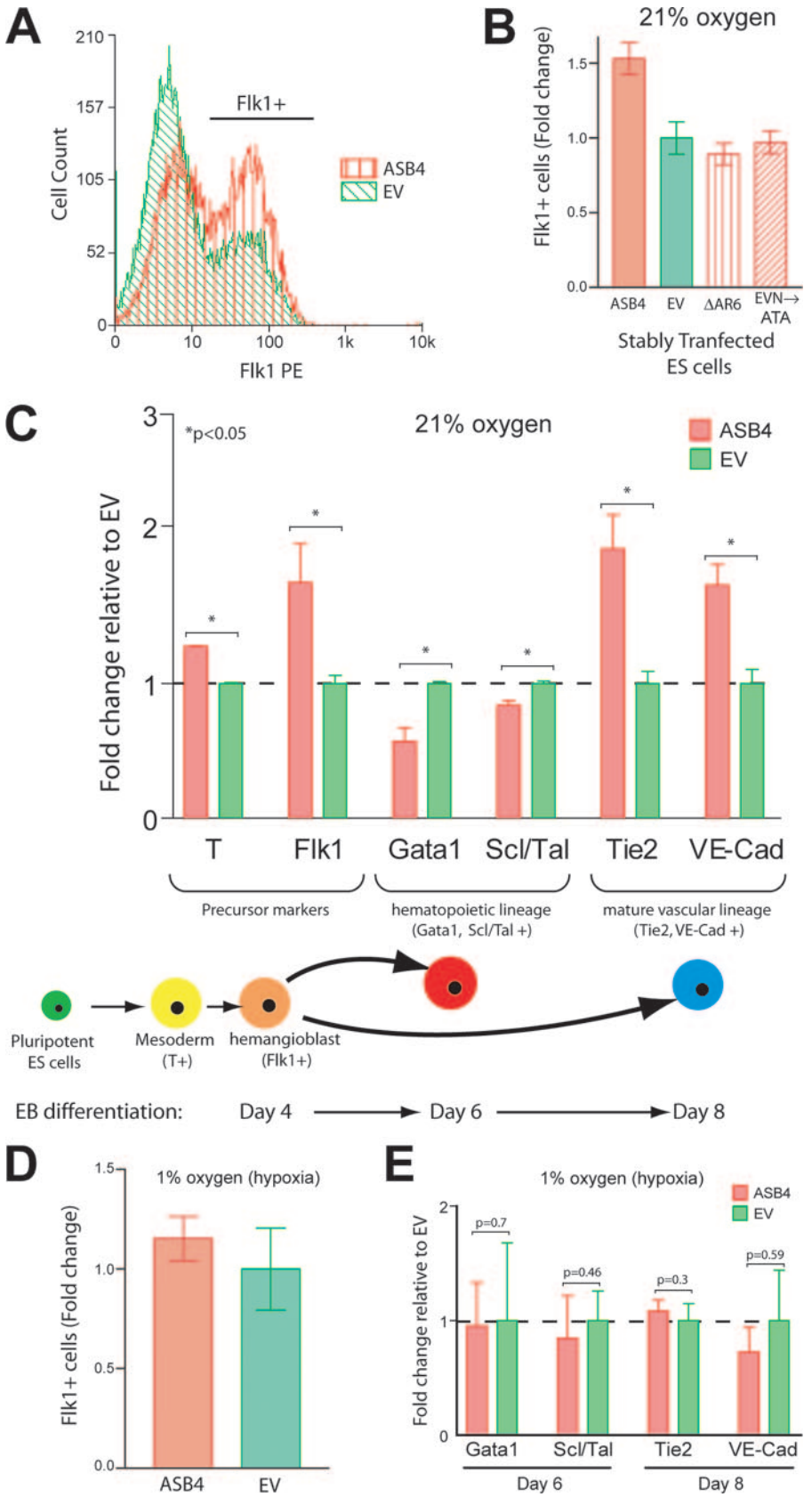

FIG. 7. ASB4 overexpression in ES cells increases the percentage of Flk1$^+$ cells and vascular commitment via an oxygen-dependent mechanism. ES cells were electroporated with constructs encoding cytomegalovirus promoter-driven 3×Flag-ASB4, unhydroxylatable ASB4 mutants (ΔAR6 and EVN→ATA), or the vector alone (EV), and stably expressing clones were selected for by culture in G418 for 14 days. Positive clones were

inherently resistant to RNAi-mediated downregulation.) After 14 days, surviving colonies were picked and expanded and expression was confirmed by immunoblotting. Multiple clones were chosen for initial experiments to control for nonspecific effects due to random integration. Upon differentiation, ASB4-expressing clones, but not unhydroxylatable mutants, demonstrated a significant increase in $Flk1^+$ cells at 96 h of differentiation compared to EV clones (Fig. 7A and B), indicating that ASB4 expression leads to an expansion of the hematovascular lineage and that this effect is dependent on the hydroxylated Asn 246 in AR6. To examine the causes of this $Flk1^+$ cell increase and to investigate the ramifications of this increase for downstream lineage commitment, real-time RT-PCR analysis was performed with stage- and lineage-restricted genes. Since $Flk1^+$ cells arise from mesoderm cells during differentiation, we investigated the overall levels of brachyury (T) expression as a marker for mesoderm. At day 4 of differentiation, brachyury levels were slightly, but significantly, increased in ASB4-expressing clones, suggesting increased mesodermal commitment (Fig. 7C). Since $Flk1^+$ cells are progenitors for both hematopoietic and vascular cells in this system, we investigated the global expression levels of a variety of hematopoietic (Gata1, Scl/Tal) and vascular (Tie2, VE-cadherin) markers. All of these markers were tested at time points representing the peak of their expression in this system (day 6 for hematopoietic markers, day 8 for vascular makers). Interestingly, compared to EV clones, ASB4-expressing clones exhibited increased expression of vascular markers and decreased expression of hematopoietic markers, suggesting that enforced expression of ASB4 causes preferential commitment of stem cells to the vascular lineage (Fig. 7C). Together, these data suggest that ASB4 induces the formation of vascular precursors from mesoderm and promotes commitment to the vascular lineage.

On the basis of our hypothesis that ASB4 is likely to be regulated by oxygen concentration, we predicted that its effects on vascular lineage commitment are oxygen dependent. To test this hypothesis, we differentiated the stably transfected ES cells described above under hypoxic conditions (1% atmospheric oxygen). The kinetics of differentiation are similar to normoxic differentiation (data not shown), so the same time points were used for analysis of lineage-restricted markers. Interestingly, the differences in the commitment to the $Flk1^+$ cell population, as well as the expression of hematopoietic and vascular lineage-specific markers observed with ASB4 overexpression under normoxic conditions, were completely abrogated by hypoxic treatment (Fig. 7D and E), indicating that the ability of ASB4 to promote the differentiation or maturation of the endothelial lineage is oxygen dependent and is inhibited by hypoxia.

DISCUSSION

In the present study, we show for the first time that ASB4 (i) is a substrate recognition molecule of an E3 ubiquitin ligase complex, (ii) is highly expressed in the vascular lineage during development, (iii) functions to promote differentiation and maturation of the vascular lineage by an oxygen-dependent mechanism, and (iv) is regulated by FIH-mediated hydroxylation. These data are consistent with our model in which ASB4 functions in an oxygen-dependent manner in order to promote endothelial differentiation and/or maturation in response to increasing oxygen levels during early vascular development.

ASB4 is a member of the SOCS superfamily, whose members function as the substrate recognition molecules of a cullin-based E3 ubiquitin ligase complex. The list of characterized E3 ubiquitin ligase proteins is rapidly expanding, and recent studies have uncovered a novel role for ubiquitin ligases during endothelial differentiation and maturation. HIF and Notch family members are critical for proper vascular development, especially during endothelial remodeling, and both families are tightly regulated by ubiquitin-mediated proteasomal degradation. For example, VHL binds to hydroxylated HIF1α to mediate its degradation in an oxygen-dependent manner, while Fbw7, Numb, Itch, and Mind-bomb all modulate Notch signaling (1, 15–17, 25, 26, 31, 40, 45). Deficiencies of these factors result in vascular abnormalities, indicating that signal regulation via the ubiquitin-proteasome system is critical for proper vascular development (10, 11, 44, 45). The endothelium-restricted expression of ASB4 described in this report further emphasizes the important role of the ubiquitin-proteasome system in modulating endothelial biology during embryogenesis.

The vascular expression of ASB4 is not only spatially restricted to the primitive endothelium but is also tightly temporally regulated. ASB4 is maximally expressed in both the embryonic vasculature and the developing placenta from E9.5 to E10.5 but is then quickly downregulated, demonstrating that ASB4 function in the vasculature is temporally confined. Notably, this brief period of high ASB4 expression coincides with rapid and drastic changes in embryonic oxygen levels. As the placenta forms between E9.5 and E10.5, oxygen delivery to the embryo quickly changes from passive diffusion through the multiple cell layers of the decidua and the embryo to maternal-fetal blood gas exchange across thin placental membranes (4). Intraembryonic oxygen tension quickly rises, and the endothe-

isolated, expanded, and used for differentiation experiments as previously described. (A and B) FACS analysis of 96-h differentiated embryoid bodies (EBs) shows a drastic increase in $Flk1^+$ cells in ASB4-expressing clones but not in clones expressing unhydroxylatable mutants. Results in panel A are representative of three independent experiments. Results in panel B represent averages of three independent clones in three independent differentiation experiments. $Flk1^+$ cells in ASB4-expressing clones were normalized to EV clones in each experiment. (C) Real-time RT-PCR analysis of differentiated embryoid bodies was used to determine the lineage commitment of ASB4-expressing ES cells. Compared with EV cells, 96-h differentiated ASB4-expressing ES cells show increased expression of a marker of mesoderm commitment (brachyury [T]) and of a marker of early vascular lineage commitment (Flk1). At day 6, ASB4-expressing ES cells show decreased expression of hematopoietic lineage markers (Gata1, Scl/Tal), and at day 8, they show increased expression of vascular markers (Tie2, VE-cadherin [VE-Cad]). Results represent averages of three independent biologic replicates. (D and E) Embryoid bodies stably expressing either ASB4 or EV were differentiated under hypoxic conditions (1% oxygen) and analyzed via FACS and real-time PCR as described for panels B and C.

lium must transduce these environmental cues into an appropriate biologic response. ASB4 is uniquely expressed temporally and spatially to play a role in the unique response of the endothelium to changing oxygen concentrations (41). Interestingly, ASB4 is conserved in animals as distant as zebra fish, but the hydroxylated asparagine is only conserved in animals that develop within a placenta or an egg. Zebra fish, which develop externally and thus have less drastic changes in oxygen tension during development, show no conservation of this region.

Our data indicate that one of the ramifications of ASB4 function is to increase the differentiation and maturation of the vascular lineage in an oxygen-dependent manner, suggesting that ASB4 may function to coordinate endothelial differentiation or maturation in the face of changing oxygen levels. This is especially intriguing considering the role of oxygen concentration on placental vascular development. The allantois, which has been shown to harbor mesoderm-derived vasculogenic cells (6), makes contact with the chorion around E8.5 to initiate placental vascularization (reviewed in references 4 and 42). During this process, a subset of trophoblast cells migrate into the uterine wall, proliferate, and differentiate into endothelium-like cytotrophoblast cells that line the maternal blood vessels to facilitate maternal-fetal blood gas exchange. Oxygen tension is critical in this process. Early on, hypoxia activates cytotrophoblast proliferation and invasion of the uterine tissues, but as these cells reach the highly oxygenated maternal blood vessels, the high oxygen levels inhibit proliferation and promote their differentiation into an endothelium-like phenotype (8, 9). It is interesting that overall ASB4 expression levels in whole allantoides and placentas are initially high and decrease concomitantly with vessel maturation and increasing oxygen tensions, suggesting that ASB4 may function to modulate placental cellular differentiation in response to changing oxygen microenvironments.

ASB4 is hydroxylated by FIH, which provides a mechanism for the ASB4-mediated oxygen-dependent modulation of vascular differentiation or maturation. The hydroxylation activity of FIH is known to be proportional to the oxygen concentration, and in this way, ASB4 hydroxylation may be an early step in the transduction of environmental oxygen cues to appropriate biological responses. Since hydroxylation has been shown to affect protein-protein interactions between the SOCS family member VHL and its ubiquitination substrate HIF1α, and since we were unable to detect any differences in ASB4 expression, subcellular localization, or autoubiquitination under hypoxic conditions (data not shown), we predict that the functional ramification of ASB4 hydroxylation is to modulate ASB4 binding to and degradation of substrate protein(s). Until recently, the only known intracellular hydroxylated proteins were HIF1α and HIF2α subunits and it was thus supposed that the cellular response to hypoxia was largely dependent upon HIF-mediated transcriptional upregulation of hypoxia response genes such as those for VEGF and GLUT-1 (3, 32). However, our data indicate that ASB4 is a member of a currently limited number of non-HIF FIH hydroxylation substrates and suggest that the mechanisms of the cellular hypoxic response may be much broader and more complex than initially suspected.

Whereas HIF1α subunits are responsible for the transcriptional response to hypoxia, ASB4 may represent a major component of the cellular posttranslational response to changing oxygen levels. Compared to transcriptional upregulation, posttranslational ubiquitination is much more rapid and enables a faster cellular response without the lag time associated with transcriptional activation and protein synthesis. For example, the ubiquitin-proteasome system extensively regulates the cell cycle, a process governed by dynamic changes in protein levels (35). Thus, oxygen-dependent ubiquitin ligase activity of ASB4 may allow the cell to respond rapidly to the quickly changing oxygen microenvironments that are found immediately following the initiation of placental blood gas exchange. Furthermore, unlike HIF1α, which is expressed in nearly all cell types, cell-specific expression of hydroxylated proteins such as ASB4 allows cell type-specific responses to changing oxygen levels. In this case, ASB4 may function to initiate rapid endothelial differentiation in response to quickly rising oxygen tensions during development. These data provide new insights into the mechanistic complexity of oxygen sensing in mammalian cells and suggest that endothelial and other cell types may mount unique responses to changing oxygen tensions during development through oxygen-dependent modulation of the ubiquitin-proteasome system.

ACKNOWLEDGMENTS

Thanks go to W. Alexander for ASB1/ASB4 pEF1 constructs; Y. Xiong for Cul2, Cul5, and Roc1 antibodies; C. Scarlett for mass spectrometric expertise; B. Temple for structural modeling; and M. Willis, R. Kelley, J. Schisler, and P. Charles for manuscript critiques.

C.P. is an Established Investigator of the American Heart Association and a Burroughs Wellcome Fund Clinician Scientist in Translational Research. This work was supported by American Heart Association predoctoral fellowship 0515350U to J.F. and National Institutes of Health grants HL 61656, HL 03658, and HL 072347 to C.P.

REFERENCES

1. **Chastagner, P., A. Israel, and C. Brou.** 2006. Itch/AIP4 mediates Deltex degradation through the formation of K29-linked polyubiquitin chains. EMBO Rep. **7:**1147–1153.
2. **Chung, A. S., Y. J. Guan, Z. L. Yuan, J. E. Albina, and Y. E. Chin.** 2005. Ankyrin repeat and SOCS box 3 (ASB3) mediates ubiquitination and degradation of tumor necrosis factor receptor II. Mol. Cell. Biol. **25:**4716–4726.
3. **Cockman, M. E., D. E. Lancaster, I. P. Stolze, K. S. Hewitson, M. A. McDonough, M. L. Coleman, C. H. Coles, X. Yu, R. T. Hay, S. C. Ley, C. W. Pugh, N. J. Oldham, N. Masson, C. J. Schofield, and P. J. Ratcliffe.** 2006. Posttranslational hydroxylation of ankyrin repeats in IκB proteins by the hypoxia-inducible factor (HIF) asparaginyl hydroxylase, factor inhibiting HIF (FIH). Proc. Natl. Acad. Sci. USA **103:**14767–14772.
4. **Cross, J. C.** 2006. Placental function in development and disease. Reprod. Fertil. Dev. **18:**71–76.
5. **Debrincat, M. A., J. G. Zhang, T. A. Willson, J. Silke, L. M. Connolly, R. J. Simpson, W. S. Alexander, N. A. Nicola, B. T. Kile, and D. J. Hilton.** 2007. Ankyrin repeat and suppressors of cytokine signaling box containing protein Asb-9 targets creatine kinase B for degradation. J. Biol. Chem. **282:**4728–4737.
6. **Downs, K. M., S. Gifford, M. Blahnik, and R. L. Gardner.** 1998. Vascularization in the murine allantois occurs by vasculogenesis without accompanying erythropoiesis. Development **125:**4507–4520.
7. **Elkins, J. M., K. S. Hewitson, L. A. McNeill, J. F. Seibel, I. Schlemminger, C. W. Pugh, P. J. Ratcliffe, and C. J. Schofield.** 2003. Structure of factor-inhibiting hypoxia-inducible factor (HIF) reveals mechanism of oxidative modification of HIF-1α. J. Biol. Chem. **278:**1802–1806.
8. **Genbacev, O., R. Joslin, C. H. Damsky, B. M. Polliotti, and S. J. Fisher.** 1996. Hypoxia alters early gestation human cytotrophoblast differentiation/invasion in vitro and models the placental defects that occur in preeclampsia. J. Clin. Investig. **97:**540–550.
9. **Genbacev, O., Y. Zhou, J. W. Ludlow, and S. J. Fisher.** 1997. Regulation of human placental development by oxygen tension. Science **277:**1669–1672.
10. **Gnarra, J. R., J. M. Ward, F. D. Porter, J. R. Wagner, D. E. Devor, A. Grinberg, M. R. Emmert-Buck, H. Westphal, R. D. Klausner, and W. M. Linehan.** 1997. Defective placental vasculogenesis causes embryonic lethality in VHL-deficient mice. Proc. Natl. Acad. Sci. USA **94:**9102–9107.

11. **Haase, V. H., J. N. Glickman, M. Socolovsky, and R. Jaenisch.** 2001. Vascular tumors in livers with targeted inactivation of the von Hippel-Lindau tumor suppressor. Proc. Natl. Acad. Sci. USA **98:**1583–1588.
12. **Heuzé, M. L., F. C. Guibal, C. A. Banks, J. W. Conaway, R. C. Conaway, Y. E. Cayre, A. Benecke, and P. G. Lutz.** 2005. ASB2 is an elongin BC-interacting protein that can assemble with cullin 5 and Rbx1 to reconstitute an E3 ubiquitin ligase complex. J. Biol. Chem. **280:**5468–5474.
13. **Hilton, D. J., R. T. Richardson, W. S. Alexander, E. M. Viney, T. A. Willson, N. S. Sprigg, R. Starr, S. E. Nicholson, D. Metcalf, and N. A. Nicola.** 1998. Twenty proteins containing a C-terminal SOCS box form five structural classes. Proc. Natl. Acad. Sci. USA **95:**114–119.
14. **Huber, T. L., V. Kouskoff, H. J. Fehling, J. Palis, and G. Keller.** 2004. Haemangioblast commitment is initiated in the primitive streak of the mouse embryo. Nature **432:**625–630.
15. **Itoh, M., C. H. Kim, G. Palardy, T. Oda, Y. J. Jiang, D. Maust, S. Y. Yeo, K. Lorick, G. J. Wright, L. Ariza-McNaughton, A. M. Weissman, J. Lewis, S. C. Chandrasekharappa, and A. B. Chitnis.** 2003. Mind bomb is a ubiquitin ligase that is essential for efficient activation of Notch signaling by Delta. Dev. Cell **4:**67–82.
16. **Ivan, M., K. Kondo, H. Yang, W. Kim, J. Valiando, M. Ohh, A. Salic, J. M. Asara, W. S. Lane, and W. G. Kaelin, Jr.** 2001. HIFα targeted for VHL-mediated destruction by proline hydroxylation: implications for O_2 sensing. Science **292:**464–468.
17. **Jaakkola, P., D. R. Mole, Y. M. Tian, M. I. Wilson, J. Gielbert, S. J. Gaskell, A. Kriegsheim, H. F. Hebestreit, M. Mukherji, C. J. Schofield, P. H. Maxwell, C. W. Pugh, and P. J. Ratcliffe.** 2001. Targeting of HIF-α to the von Hippel-Lindau ubiquitylation complex by O2-regulated prolyl hydroxylation. Science **292:**468–472.
18. **Kamura, T., K. Maenaka, S. Kotoshiba, M. Matsumoto, D. Kohda, R. C. Conaway, J. W. Conaway, and K. I. Nakayama.** 2004. VHL-box and SOCS-box domains determine binding specificity for Cul2-Rbx1 and Cul5-Rbx2 modules of ubiquitin ligases. Genes Dev. **18:**3055–3065.
19. **Kamura, T., S. Sato, D. Haque, L. Liu, W. G. Kaelin, Jr., R. C. Conaway, and J. W. Conaway.** 1998. The elongin BC complex interacts with the conserved SOCS-box motif present in members of the SOCS, ras, WD-40 repeat, and ankyrin repeat families. Genes Dev. **12:**3872–3881.
20. **Kattman, S. J., T. L. Huber, and G. M. Keller.** 2006. Multipotent flk-1^+ cardiovascular progenitor cells give rise to the cardiomyocyte, endothelial, and vascular smooth muscle lineages. Dev. Cell **11:**723–732.
21. **Kile, B. T., B. A. Schulman, W. S. Alexander, N. A. Nicola, H. M. Martin, and D. J. Hilton.** 2002. The SOCS box: a tale of destruction and degradation. Trends Biochem. Sci. **27:**235–241.
22. **Kile, B. T., E. M. Viney, T. A. Willson, T. C. Brodnicki, M. R. Cancilla, A. S. Herlihy, B. A. Croker, M. Baca, N. A. Nicola, D. J. Hilton, and W. S. Alexander.** 2000. Cloning and characterization of the genes encoding the ankyrin repeat and SOCS box-containing proteins Asb-1, Asb-2, Asb-3 and Asb-4. Gene **258:**31–41.
23. **Kohroki, J., T. Nishiyama, T. Nakamura, and Y. Masuho.** 2005. ASB proteins interact with cullin 5 and Rbx2 to form E3 ubiquitin ligase complexes. FEBS Lett. **579:**6796–6802.
24. **Kondo, K., and W. G. Kaelin, Jr.** 2001. The von Hippel-Lindau tumor suppressor gene. Exp. Cell Res. **264:**117–125.
25. **Koo, B. K., K. J. Yoon, K. W. Yoo, H. S. Lim, R. Song, J. H. So, C. H. Kim, and Y. Y. Kong.** 2005. Mind bomb-2 is an E3 ligase for Notch ligand. J. Biol. Chem. **280:**22335–22342.
26. **Lai, E. C., F. Roegiers, X. Qin, Y. N. Jan, and G. M. Rubin.** 2005. The ubiquitin ligase Drosophila Mind bomb promotes Notch signaling by regulating the localization and activity of Serrate and Delta. Development **132:**2319–2332.
27. **Lando, D., D. J. Peet, D. A. Whelan, J. J. Gorman, and M. L. Whitelaw.** 2002. Asparagine hydroxylation of the HIF transactivation domain a hypoxic switch. Science **295:**858–861.
28. **Li, H. H., V. Kedar, C. Zhang, H. McDonough, R. Arya, D. Z. Wang, and C. Patterson.** 2004. Atrogin-1/muscle atrophy F-box inhibits calcineurin-dependent cardiac hypertrophy by participating in an SCF ubiquitin ligase complex. J. Clin. Investig. **114:**1058–1071.
29. **Linke, S., C. Stojkoski, R. J. Kewley, G. W. Booker, M. L. Whitelaw, and D. J. Peet.** 2004. Substrate requirements of the oxygen-sensing asparaginyl hydroxylase factor-inhibiting hypoxia-inducible factor. J. Biol. Chem. **279:**14391–14397.
30. **Maxwell, P. H., and P. J. Ratcliffe.** 2002. Oxygen sensors and angiogenesis. Semin. Cell Dev. Biol. **13:**29–37.
31. **McGill, M. A., and C. J. McGlade.** 2003. Mammalian numb proteins promote Notch1 receptor ubiquitination and degradation of the Notch1 intracellular domain. J. Biol. Chem. **278:**23196–23203.
32. **Metzen, E., and P. J. Ratcliffe.** 2004. HIF hydroxylation and cellular oxygen sensing. Biol. Chem. **385:**223–230.
33. **Mosavi, L. K., T. J. Cammett, D. C. Desrosiers, and Z. Y. Peng.** 2004. The ankyrin repeat as molecular architecture for protein recognition. Protein Sci. **13:**1435–1448.
34. **Moser, M., O. Binder, Y. Wu, J. Aitsebaomo, R. Ren, C. Bode, V. L. Bautch, F. L. Conlon, and C. Patterson.** 2003. BMPER, a novel endothelial cell precursor-derived protein, antagonizes bone morphogenetic protein signaling and endothelial cell differentiation. Mol. Cell. Biol. **23:**5664–5679.
35. **Nakayama, K. I., and K. Nakayama.** 2006. Ubiquitin ligases: cell-cycle control and cancer. Nat. Rev. Cancer **6:**369–381.
36. **Ohta, T., J. J. Michel, A. J. Schottelius, and Y. Xiong.** 1999. ROC1, a homolog of APC11, represents a family of cullin partners with an associated ubiquitin ligase activity. Mol. Cell **3:**535–541.
37. **Pan, Y., K. D. Mansfield, C. C. Bertozzi, V. Rudenko, D. A. Chan, A. J. Giaccia, and M. C. Simon.** 2007. Multiple factors affecting cellular redox status and energy metabolism modulate hypoxia-inducible factor prolyl hydroxylase activity in vivo and in vitro. Mol. Cell. Biol. **27:**912–925.
38. **Parker, C. E., V. Mocanu, M. R. Warren, S. F. Greer, and C. H. Borchers.** 2005. Mass spectrometric determination of protein ubiquitination. Methods Mol. Biol. **301:**153–173.
39. **Pugh, C. W., and P. J. Ratcliffe.** 2003. The von Hippel-Lindau tumor suppressor, hypoxia-inducible factor-1 (HIF-1) degradation, and cancer pathogenesis. Semin. Cancer Biol. **13:**83–89.
40. **Qiu, L., C. Joazeiro, N. Fang, H. Y. Wang, C. Elly, Y. Altman, D. Fang, T. Hunter, and Y. C. Liu.** 2000. Recognition and ubiquitination of Notch by Itch, a hect-type E3 ubiquitin ligase. J. Biol. Chem. **275:**35734–35737.
41. **Ramírez-Bergeron, D. L., A. Runge, K. D. Dahl, H. J. Fehling, G. Keller, and M. C. Simon.** 2004. Hypoxia affects mesoderm and enhances hemangioblast specification during early development. Development **131:**4623–4634.
42. **Rossant, J., and J. C. Cross.** 2001. Placental development: lessons from mouse mutants. Nat. Rev. Genet. **2:**538–548.
43. **Sedgwick, S. G., and S. J. Smerdon.** 1999. The ankyrin repeat: a diversity of interactions on a common structural framework. Trends Biochem. Sci. **24:**311–316.
44. **Tetzlaff, M. T., W. Yu, M. Li, P. Zhang, M. Finegold, K. Mahon, J. W. Harper, R. J. Schwartz, and S. J. Elledge.** 2004. Defective cardiovascular development and elevated cyclin E and Notch proteins in mice lacking the Fbw7 F-box protein. Proc. Natl. Acad. Sci. USA **101:**3338–3345.
45. **Tsunematsu, R., K. Nakayama, Y. Oike, M. Nishiyama, N. Ishida, S. Hatakeyama, Y. Bessho, R. Kageyama, T. Suda, and K. I. Nakayama.** 2004. Mouse Fbw7/Sel-10/Cdc4 is required for notch degradation during vascular development. J. Biol. Chem. **279:**9417–9423.
46. **Wang, H., P. C. Charles, Y. Wu, R. Ren, X. Pi, M. Moser, M. Barshishat-Kupper, J. S. Rubin, C. Perou, V. Bautch, and C. Patterson.** 2006. Gene expression profile signatures indicate a role for Wnt signaling in endothelial commitment from embryonic stem cells. Circ. Res. **98:**1331–1339.
47. **Wilcox, A., K. D. Katsanakis, F. Bheda, and T. S. Pillay.** 2004. Asb6, an adipocyte-specific ankyrin and SOCS box protein, interacts with APS to enable recruitment of elongins B and C to the insulin receptor signaling complex. J. Biol. Chem. **279:**38881–38888.